Journal for ImmunoTherapy of Cancer

Multiple TMA-aided CRISPR/Cas13a platform for highly sensitive detection of IL-15 to predict immunotherapeutic response in nasopharyngeal carcinoma

Ya-Xian Wu,[1] Shan Xing,[1] Yu Wang,[2] Bo-Yu Tian,[1] Meng Wu,[1] Xue-Ping Wang ,[1] Qi Huang,[1] Xia He,[1] Shu-Lin Chen,[1] Xiao-Hui Li,[1] Mu-Sheng Zeng,[2] Wan-Li Liu [1]

To cite: Wu Y-X, Xing S, Wang Y, *et al*. Multiple TMA-aided CRISPR/Cas13a platform for highly sensitive detection of IL-15 to predict immunotherapeutic response in nasopharyngeal carcinoma. *Journal for ImmunoTherapy of Cancer* 2023;**11**:e006552. doi:10.1136/jitc-2022-006552

► Additional supplemental material is published online only. To view, please visit the journal online (http://dx.doi.org/10.1136/jitc-2022-006552).

Y-XW, SX and YW contributed equally.

Accepted 13 July 2023

Check for updates

© Author(s) (or their employer(s)) 2023. Re-use permitted under CC BY-NC. No commercial re-use. See rights and permissions. Published by BMJ.

For numbered affiliations see end of article.

Correspondence to
PhD Wan-Li Liu;
liuwl@sysucc.org.cn

Prof Mu-Sheng Zeng;
zengmsh@sysucc.org.cn

ABSTRACT

Background Immune checkpoint inhibitors (ICIs)-based treatments have been recommended as the first line for refractory recurrent and/or metastatic nasopharyngeal carcinoma (NPC) patients, yet responses vary, and predictive biomarkers are urgently needed. We selected serum interleukin-15 (sIL-15) out of four interleukins as a candidate biomarker, while most patients' sIL-15 levels were too low to be detected by conventional methods, so it was necessary to construct a highly sensitive method to detect sIL-15 in order to select NPC patients who would benefit most or least from ICIs.

Methods Combining a primer exchange reaction (PER), transcription-mediated amplification (TMA), and a immuno-PER-TMA-CRISPR/Cas13a system, we developed a novel multiple signal amplification platform with a detection limit of 32 fg/mL, making it 153-fold more sensitive than ELISA.

Results This platform demonstrated high specificity, repeatability, and versatility. When applied to two independent cohorts of 130 NPC sera, the predictive value of sIL-15 was accurate in both cohorts (area under the curve: training, 0.882; validation, 0.898). Additionally, lower sIL-15 levels were correlated with poorer progression-free survival (training, HR: 0.080, p<0.0001; validation, HR: 0.053, p<0.0001).

Conclusion This work proposes a simple and sensitive approach for sIL-15 detection to provide insights for personalized immunotherapy of NPC patients.

WHAT IS ALREADY KNOWN ON THIS TOPIC

⇒ Not all patients with nasopharyngeal carcinoma (NPC) will obtain the same clinical benefit from immunotherapy, so finding effective predictive biomarkers is necessary. IL-15, which improves the efficacy of immunotherapy, could be a potential predictive biomarker, while most patients' serum IL-15 levels were too low to be detected by conventional methods.

WHAT THIS STUDY ADDS

⇒ This study developed a highly sensitive platform for serum IL-15 detection using a novel multiple transcription-mediated amplification (TMA)-assisted CRISPR/Cas13a signal amplification strategy by combining a primer exchange reaction, TMA, and a CRISPR/Cas13a system. We demonstrated that high baseline serum IL-15 levels were associated with a better response to anti-PD1 antibody therapy in recurrent and/or metastasis NPC patients.

HOW THIS STUDY MIGHT AFFECT RESEARCH, PRACTICE OR POLICY

⇒ These findings suggest that baseline serum IL-15 levels could be incorporated into the guidance of individualized disease management for NPC patients in the era of immunotherapy.

INTRODUCTION

Immune checkpoint inhibitors (ICIs) based on programmed death-1/programmed death ligand-1 (PD-1/PD-L1) blockade are breakthrough agents and were approved for the treatment of refractory recurrent and/or metastatic (R/M) nasopharyngeal carcinoma (NPC) in 2021 in China.[1] However, only a subset of NPC patients achieves clinical benefits, and biomarkers, especially peripheral blood biomarkers, are lacking to guide ICI-related treatment choices. The abilities of cytokines to mediate and regulate immunity have been extensively studied, and some cytokines, such as IL-8,[2 3] have been found to reflect the response to ICI-based treatment.[4–7] Interleukin (IL)-15 is a proinflammatory cytokine that stimulates the proliferation and maintenance of natural killer (NK) cells and T and B lymphocytes,[8] and it exerts antitumor effects by enhancing immunosurveillance and preventing tumor formation.[9 10] Further substantiation for the immune role of IL-15 is shown by its impact on $CD8^+$T cells, promoting and enhancing the antitumor activity of PD-1 antagonists.[11] Various preclinical approaches have indicated that IL-15 can improve the efficacy of immunotherapy.[9 10 12] However, due to the extremely low levels of

IL-15 in the peripheral blood,[13] the predictive efficacy of sIL-15 levels in anti-PD-1 treatment has not been comprehensively validated; therefore, the development of highly sensitive assays is of paramount importance.

Sandwich ELISA for detecting interleukins is currently the most widely used clinical method to measure serum IL-15 (sIL-15) levels. However, it is not sensitive enough to detect low sIL-15 concentrations in certain patients. Various amplification technologies have been designed and integrated into ELISA to overcome this limitation to achieve ultrasensitivity and a multiplexing capability.[14] Niemeyer *et al* established PCR-ELISA,[15] which converts protein signals into DNA signals and represents a great improvement compared with ELISA. However, the process of PCR-ELISA is tedious and relies on sophisticated thermal cycling devices.[16 17] Subsequently, recombinase polymerase amplification (RPA)-ELISA was introduced; this approach eliminates the thermal cycling step[18] but has a high cost and easily produces false positives caused by contamination. Recently, clustered regularly interspaced short palindromic repeats–CRISPR/associated protein (CRISPR/Cas) systems, such as the Cas12, Cas13, and Cas14 systems, have been leveraged for ultrasensitive nucleic acid detection.[19–21] In these systems, the recognition of a target DNA or RNA by CRISPR RNA (crRNA) leads to the Cas protein switching to an active state, wherein the single-stranded DNA (ssDNA) or single-stranded RNA (ssRNA) substrate is cleaved in a nonspecific way and simultaneously releases the signal.[22–25] Joung *et al*[21] developed a nucleic acid diagnostic platform called SHERLOCK, which uses the CRISPR/Cas13a system for highly sensitive and straightforward detection of Zika, dengue, and SARS-CoV-2. Fozouni *et al*[26] developed a quantitative detection method for SARS-CoV-2 RNA without preamplification using CRISPR/Cas13a integrated with a mobile phone. Furthermore, the CRISPR/Cas system has been introduced as a signal amplification strategy for microprotein determination. Previously, we[27 28] established aptamer ELISA-based CRISPR/Cas assays to detect trace proteins on extracellular vesicles.[29] Nevertheless, the lack of reported IL-15 aptamers limits the application of this approach. Another group introduced a CRISPR/Cas13a signal amplification-linked ELISA for microprotein detection,[30] which achieved double signal amplification based on transcription-mediated amplification (TMA) and the CRISPR/Cas13a system. However, the detection sensitivity of this method needs to be improved.

Recently, primer exchange reaction (PER) cascades were established by Kishi *et al*[31]; these cascades isothermally generate arbitrary ssDNA concatemers with the help of a DNA primer, a hairpin, and a strand-displacing polymerase in one-step amplification. Different from other enzyme-driven amplification methods, such as PCR,[32 33] rolling circle amplification,[34 35] and polymerase–exonuclease/nickase reaction,[36] which are limited to producing identical copies of fixed sequences, PER provides a general method for autonomously synthesizing user-prescribed concatemers with repeat units.[37 38] Due to its superior amplification capability, this technique has been applied to imaging proteins[39] and nucleic acids[40] in cells and tissues. Additionally, to further improve sensitivity and specificity, PER cascades have been integrated with the CRISPR/Cas12a system for ribonuclease H (RNase H) activity detection[41] and SARS-CoV-2 RNA detection.[42] Further efforts to make full use of PER by combining it with other amplification methods are being considered.

In this work, we selected sIL-15 as a candidate biomarker by examining the predictive effect of four kinds of interleukins (IL-15, IL-2, IL-8, and IL-12) by ELISA on the response to ICI-based therapy in a discovery set of 62 NPC patients. However, the levels of sIL-15 in quite a few NPC patients were undetectable by ELISA. To enhance the detection limit, we developed a highly sensitive fluorescence sensing strategy for sIL-15 detection based on specific immune recognition and a PER-assisted multiple TMA-CRISPR/Cas13a signal amplification strategy, termed immuno-PER-TMA-CRISPR/Cas13a (iPTC). This platform could quantitatively detect sIL-15 with a detection limit of 32 fg/mL, making it 153-fold more sensitive than ELISA. We further revealed that baseline sIL-15 levels were associated with response and outcome for ICI-based treatment in both the training and validation cohorts. The overall results revealed that low baseline sIL-15 levels detected by the iPTC platform were associated with a less favorable outcome for ICI-based treatment.

MATERIAL AND METHODS

Materials

All oligonucleotides purified by high-performance liquid chromatography were obtained from Sangon Biotechnology (Shanghai, China). The corresponding DNA sequences and modifications are shown in online supplemental table 1. Bst DNA Polymerase, Large Fragment, was purchased from New England Biolabs (Massachusetts, USA; M0275L). dATP, dTTP, and dCTP were purchased from G-CLONE (Beijing, China; RE0081; RE0082; RE0083). The HiScribe T7 High Yield RNA Synthesis Kit was purchased from New England Biolabs (E2040S). The v2 reporter was purchased from Thermo Scientific (Massachusetts, USA; 4479769). Streptavidin-coated magnetic beads (SA@MBs) were acquired from Roche. The E.Z.N.A. A Cycle Pure Kit was purchased from Omega Bio-Tek (Georgia, USAs; D6492). The LbuCas13a used in this assay was expressed and purified by our laboratory, as described in previous studies.[20 26] The ELISA kits used in this assay were all purchased from Cloud-Clone (Wuhan, China). Other chemical reagents were purchased from Guangzhou Chemical Reagents Factory (Guangzhou, China). RNAase-free (RF) water was used in all experiments to prepare aqueous solutions.

Patient characteristics and serum samples

Sera from 130 pathologically confirmed NPC patients were collected at Sun Yat-sen University Cancer Center between January 1, 2020 and December 31, 2021.

Patient serum samples were all collected before the anti-PD1 treatment. TNM stage was established based on the eighth Edition of the Union for International Cancer Control/American Joint Committee on Cancer staging system for NPC. Patient characteristics are shown in online supplemental tables 2 and 3. For enrolled patients, the inclusion criteria were as follows: (1) patients over 18 years old; (2) patients must be diagnosed with R/M NPC with TNM stage identified as stage III/IV; (3) patients with another malignancy or inflammatory states, such as concurrent infections or autoimmune adverse events, and with a history of severe heart or liver disease were excluded; (4) patients received anti-PD-1 therapy (nivolumab, toripalimab or camrelizumab) plus chemotherapy (cisplatin, gemcitabine, paclitaxel); and (5) patients who were treated with anti-PD-1 treatment plus chemotherapy were followed up with radiographic tumor evaluation every 1–2 months.

In this study, we analyzed sIL-15 levels in 130 NPC patients; 87 baseline samples (64 non-progressive disease (non-PD), 23 PD) were used as a training cohort, and 43 baseline samples (32 non-PD, 11 PD) were used as a validation cohort. In the discovery set (group 1), we analyzed sIL-15, sIL-2, sIL-8, and sIL-12 in 62 NPC patients (44 non-PD, 18 PD) who were included in the training cohort. Patients were defined by Response Criteria in Solid Tumors 1.1. Based on MRI or CT findings, their responses to treatment were evaluated as a complete response (CR), a partial response (PR), stable disease (SD), or PD. During the follow-up time, patients, who ever/never developed PD, were defined as non-PD.

The serum was separated by centrifugation at 3500 rpm for 10 min at room temperature (RT) and then frozen at −80°C until use. Serum interleukin assays were performed by ELISA (IL-2, IL-8, IL-12, and IL-15) and with the iPTC platform (IL-2 and IL-15).

Preparation of biotinylated PER concatemers

Typically, 200 µL reactions were prepared in 1×PBS with final concentrations of 0.8 units per µL Bst DNA Polymerase Large Fragment; 10 mM $MgSO_4$; 600 µM each of dATP, dTTP and dCTP; 0.5 µM Hairpin aa; 0.1 µM dGTP Cleaner (5'-CCCCGAAAGTGGCCTCGGGCCTTT TGGCCCGAGGCCACTTTCG-3'); and RF water added to a total volume of 180 µL. Preincubation with 0.1 µM dGTP Cleaner for 15 min at 37°C eliminated the small amount of dGTP contamination. Then, 20 µL of 10 µM biotinylated primer was added to the system, and the reaction mixture was incubated for another 1–3 hours at 37°C. After heating at 80°C for 20 min, the polymerase was inactivated, and the reaction was terminated. The original biotinylated PER concatemers with a 1 µM final concentration were obtained. To remove proteins, short DNA fragments (<100 bp), and other contaminants, the E.Z.N.A. Cycle Pure Kit was leveraged to purify the original PER concatemers. Then, column-bound oligos were eluted with 50 µL of RF water, and the concentrations of purified biotinylated PER concatemers were measured using a Nanodrop depending on their absorption coefficient. Ultimately, a long strand of repeated domains 'a' (5'-ACAACTTAAC-3') was synthesized, and then this construct was used as a signal amplifier to hybridize with T7 promoter sequences. Biotinylated PER products could be stored at −20°C for several months. To illustrate the effects of different lengths of biotinylated ssDNA concatemers on fluorescence intensity (FI), we chose the 10-nucleotide (nt) sequence a (5'-CAACTTAAC-3') as the repeated domain and designed 3a (3 repeated a domains), 6a (6 repeated a domains) and 9a (9 repeated a domains) modified with biotin to compare biotinylated PER concatemers (approximately 250 repeated a domains).

Gel electrophoresis

The molecular weights of nucleic acids and proteins were observed by PAGE analysis. TBE-urea PAGE denaturing gels (5%) were used in most of the experiments, and gels were run in 1×TBE buffer at 150 V for 1 hour.[43] The gels were stained by silver staining or Coomassie blue staining.

Process of PTC

We designed strands that hybridized with the PER concatemer; that is, an antisense strand probe (AS probe) and an antisense 1 strand probe (AS1) were the strands that hybridized with the PER concatemer. A sense strand probe (S probe) and a sense 1 strand probe (S1) were the strands that hybridized with the AS/AS1 probe. The AS/AS1 probe and S/S1 probe generated a probe duplex containing the T7 promoter. First, biotinylated ssDNA concatemers were hybridized with the T7 promoter sequence in the AS/S probe complex, incubated at 95°C for 10 min, and then cooled to RT for 1 hour to obtain the PER-AS/S probe complex. This system was assembled by mixing 100 fM biotinylated PER, 10 pM AS/S probes, and 1×PCR buffer and adding RF water to a total of 200 µL. Then, the PER-AS/S probe complex was obtained. A 200 µL of streptavidin MBs was added to these systems and incubated at RT for 0.5 hour, followed by four washes.

The second signal amplification was T7 transcription mediated by recognition of the T7 promoters on AS/S probes. Typically, 20 µL reaction mixtures contained 5 mM ATP/GTP/CTP/UTP Mix, 1×Reaction Buffer,1 µL of T7 RNA Polymerase Mix, and AS/S probes with T7 promoters. The mixture was incubated at 37°C for 40 min to generate a mass of target RNA to activate the CRISPR/Cas13a system. For standard CRISPR/Cas13a detection, 20 µL systems were mixed with a final concentration of 200 nM LbuCas13a, 500 nM crRNA, 200 nM v2 reporter, 1×Thermo pol buffer, and 4 µL of transcription products, and then the mixture was loaded into a 384-well plate. Cleavage by CRISPR/Cas13a was performed in a fluorescent plate reader (Tecan Spark, Shanghai, China) at 37 °C for 60 min, and the FI was measured every 2 min (v2 reporter = $\lambda_{ex:}$ 485 nM; λ_{em}: 535 nM; gain=80).

sIL-15 detection by iPTC

For sIL-15 detection, standard solutions were prepared with the indicated concentration gradients for quantitative measurements. We used the IL-15 ELISA kit (Cloud-Clone, Wuhan, China, SEA061Hu) and followed the manufacturer's instructions to build a double-antibody sandwich. Briefly, 100 µL of standards and serum were added to a precoated 96-well plate and incubated at 37°C for 1 hour. Subsequently, a 100 µL of biotinylated anti-IL-15 antibody was added to each well and incubated for 1 hour at 37°C. Then, a 100 µL of streptavidin (500 ng/mL) was added and incubated at RT for 30 min. Then, a 50 µL of PER-AS/S probe hybridizations preassembled containing 2.5 nM biotinylated PER concatemers, 200 nM AS/S probes (with the T7 promoter sequences), and 1×PCR buffer were added to each well and reacted for 20 min at RT. After each binding incubation, the plate was washed at least four times with 0.05% PBST. Then, a 20 µL of T7 transcription mixtures was added to each well and incubated at 37°C for 40 min. Finally, the standard CRISPR/Cas13a protocol was performed, and the FI was obtained. All samples were assayed in triplicate.

Serum interleukin detection by conventional ELISA kits

The conventional sandwich ELISA method was used for serum interleukin determination. Concentrations of IL-15 (SEA061Hu), IL-2 (SEA073Hu), IL-8 (SEA080Hu), and IL-12 (SEA073Hu) were measured using ELISA kits (Cloud-Clone, Wuhan, China) according to the manufacturer's instructions. Briefly, a capture antibody was coated onto microwells. After incubation with 100 µL of standard or serum sample, the capture antibody bound the interleukin. Following extensive washing with PBS, a detection antibody was added to detect the captured target protein. An HRP-linked secondary antibody was then used to recognize the bound detection antibody, followed by incubation with 3,3',5,5'-tetramethylbenzidine (TMB) substrate in the dark. The reaction was terminated by adding a stop solution, and the optical density at 450 nm was measured immediately using a microplate reader.

Statistical analysis

GraphPad Prism V.9.2.0 software and Microsoft Excel were used for statistical analysis. A Mann-Whitney U test and a Kruskal-Wallis test were used to analyze the differences between two groups and three or more groups, respectively. To evaluate the value of serum interleukins (IL-15, IL-2, IL-8, and IL-12) in predicting immunotherapy response, we used receiver operating characteristic (ROC) curve analysis with the corresponding area under the curve (AUC). The maximal Youden index value was considered the cut-off value for each interleukin. Survival analysis was performed with the Kaplan-Meier method and log-rank test. All tests were two tailed, and a $p<0.05$ was considered to indicate statistical significance. Three replicates were performed to improve the statistics.

RESULTS

Identification of predictive biomarkers among sIL-15, sIL-2, sIL-12, and sIL-8

IL-15, IL-2, and IL-12 stimulate the development of memory $CD8^+$ T cells and NK cells, raising hopes that they could become valuable predictive biomarkers in tumor immunotherapy. IL-8 has been reported to reflect the response to ICI-based treatment across malignant tumors. We thus chose them as candidates. To test their potential predictive values on ICI response, we first enrolled 62 R/M NPC patients who received anti-PD-1 therapy plus chemotherapy and analyzed baseline sIL-15, sIL-2, sIL-12, and sIL-8 levels by ELISA in the discovery set (figure 1). The patients' baseline characteristics of the discovery set are shown in online supplemental table 2.

The scatter plots (figure 2A–D) show that only baseline sIL-15 levels measured by ELISA were significantly higher in the non-PD group (n=44) than in the PD group (n=18, $p<0.01$). Values did not differ significantly between these two groups in the other three interleukins. ROC curve analysis evaluated the predictive power of sIL-15 to distinguish patients with PD from patients with non-PD (figure 2E); the corresponding AUC was 0.700 (95% CI 0.570 to 0.830; p=0.0143), superior to the other three interleukins (sIL-2, 0.577; sIL-12, 0.611; and sIL-8, 0.517) (figure 2F–H). When the cut-off value was set to the optimal point (1.09 pg/mL), the performance of sIL-15 was better than that of other interleukins, with a sensitivity of 88.89% and a specificity of 52.27% (online supplemental table 4). These results indicate that sIL-15 may be a promising biomarker for predicting response and prognosis in NPC patients in the context of anti-PD-1 therapy. We also separated the prediction of ICI based on subgroups of non-PD (PR, SD) for each cytokine (IL-15, IL-8, IL-2, IL-12). The Kruskal-Wallis test (online supplemental figure 1A-D) showed that only baseline sIL-15 levels measured by ELISA had significant differences in the PR, SD, and PD patients, and the highest levels of sIL-15 were found in PR patients in all three groups (PR: n=22; median, 3.17; IQR, 0–11.44. SD: n=22; median, 0.15; IQR, 0–7.78. PD: n=18; median, 0; IQR, 0–0.16.). However, values for the other three interleukins did not differ significantly among these three groups ($p>0.05$).

The amount of sIL-15 in most NPC patients (42/62), nonetheless, was below the ELISA's minimum detection limit (limit of detection, LOD=4.92 pg/mL) method. Hence, we established a highly sensitive platform to improve the prediction performance of baseline sIL-15 further.

Construction of the iPTC platform

We thus combined the triple signal amplification approach and developed a novel platform named iPTC, which has a three-step process (figure 3): (1) Target protein capture by sandwich ELISA: in the presence of protein targets, the targets are captured by a capture antibody and recognized by a biotinylated detection antibody. (2) Protein signal conversion: biotinylated PER

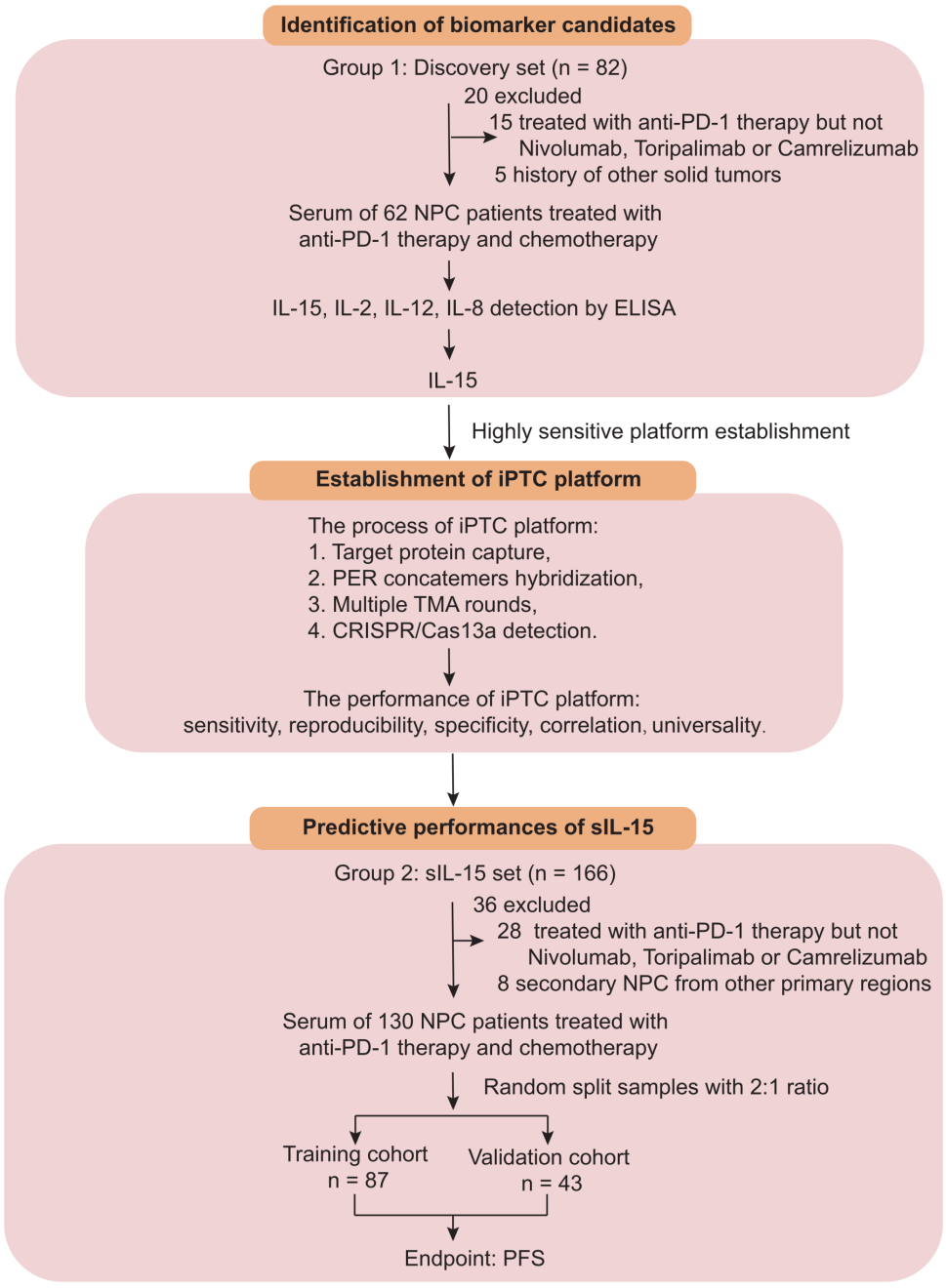


Figure 1 Overview of the study design. Top, IL-15, IL-2, IL-12, and IL-8 in the serum of 62 NPC patients were analyzed using ELISA to identify predictive biomarker candidates. Middle, process, and performance of the iPTC platform. Botton, serum IL-15 was evaluated as a novel predictive biomarker for the response to ICI-related therapy in the training cohort (n=87) and validation cohort (n=43) by the iPTC platform. The discovery set is included in the training cohort. ICI, immune checkpoint inhibitor; IL, interleukin; iPTC, immuno-PER-TMA-CRISPR/Cas13a; NPC, nasopharyngeal carcinoma; PFS, progression-free survival.

concatemers are preassembled, and then approximately one hundred double-stranded AS/S probes containing T7 promoters are hybridized to the repeated binding sites on the PER concatemers (PER-AS/S) for the next multiple TMA. After adding streptavidin, the preassembled biotinylated PER-AS/S complex is bound specifically to the antigen-antibody complex via the strong interaction between biotin and streptavidin. This step is the first signal amplification and converts the protein signals into hundreds of nucleic acid signals. (3) Multiple TMA rounds and CRISPR/Cas13a detection: T7 polymerase binds to the multiple promoters on the AS/S probes and then executes TMA to convert dsDNA into RNA. After TMA, the RNA products bind special crRNAs and activate the HPEN catalytic site of LbuCas13a. The activated Cas13a enzyme can indiscriminately cleave both the target RNA and collateral ssRNA reporter in a non-specific fashion to obtain a significantly enhanced fluorescence signal, which is proportional to the target concentration. This step involves the second signal amplification by TMA and the third signal amplification by the Cas13a enzyme. Importantly, this immunoassay platform can be

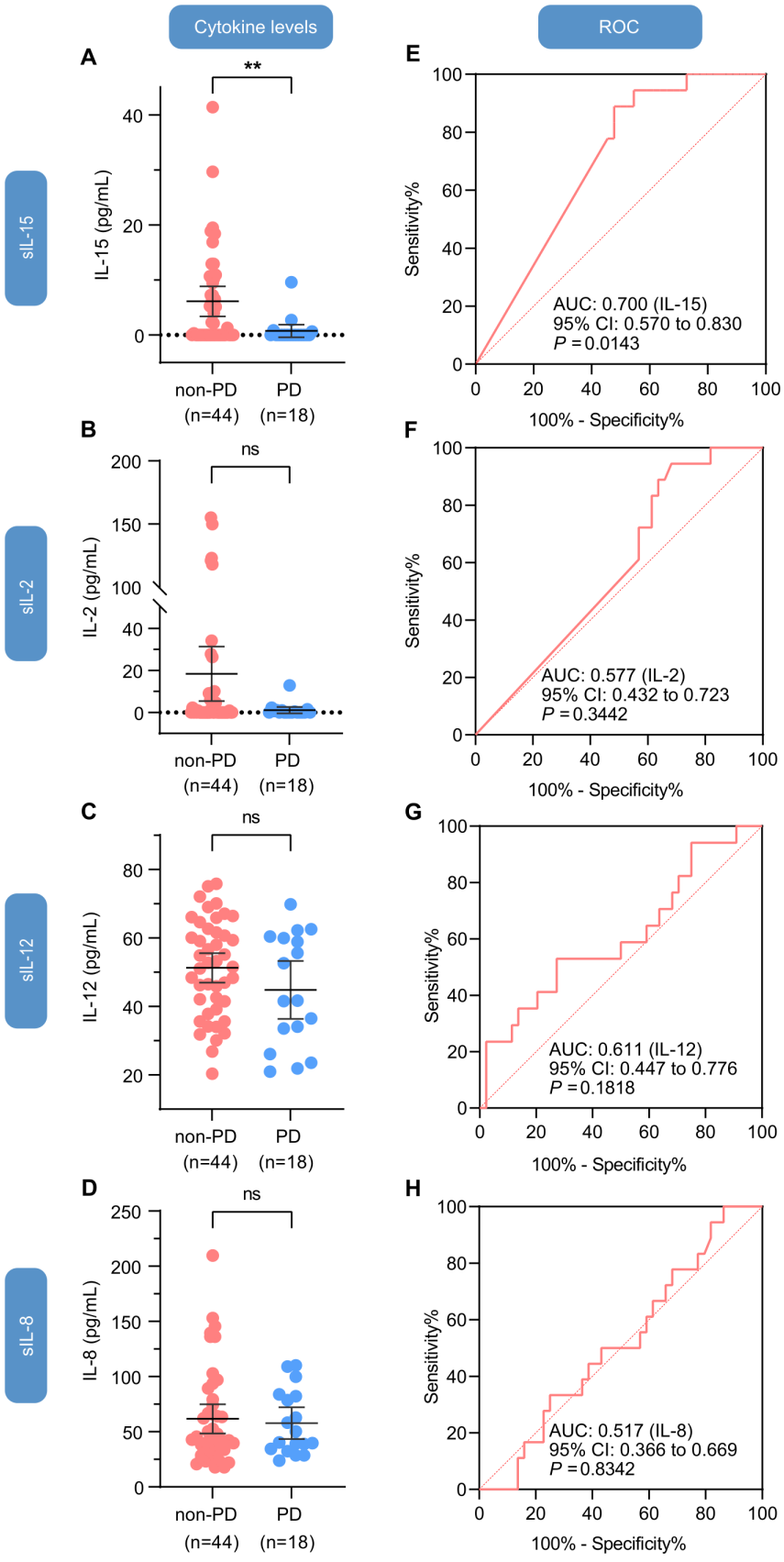


Figure 2 Prediction of ICI-related therapy response by baseline sIL-15, sIL-2, sIL-12, and sIL-8. (A–D) Scatter plots of sIL-15, sIL-2, sIL-12, and sIL-8 levels in non-PD and PD patients measured by ELISA. The two groups were statistically compared by the Kruskal-Wallis test: ** and ns represent p<0.01, p>0.05, respectively. (E–H) ROC curve analysis evaluating the predictive power of sIL-15, sIL-2, sIL-12, and sIL-8 levels in differentiating PD patients from non-PD patients, with the corresponding AUC. AUC, area under the curve; PD, progressive disease; ROC, receiver operating characteristic; sIL-15, serum interleukin-15.

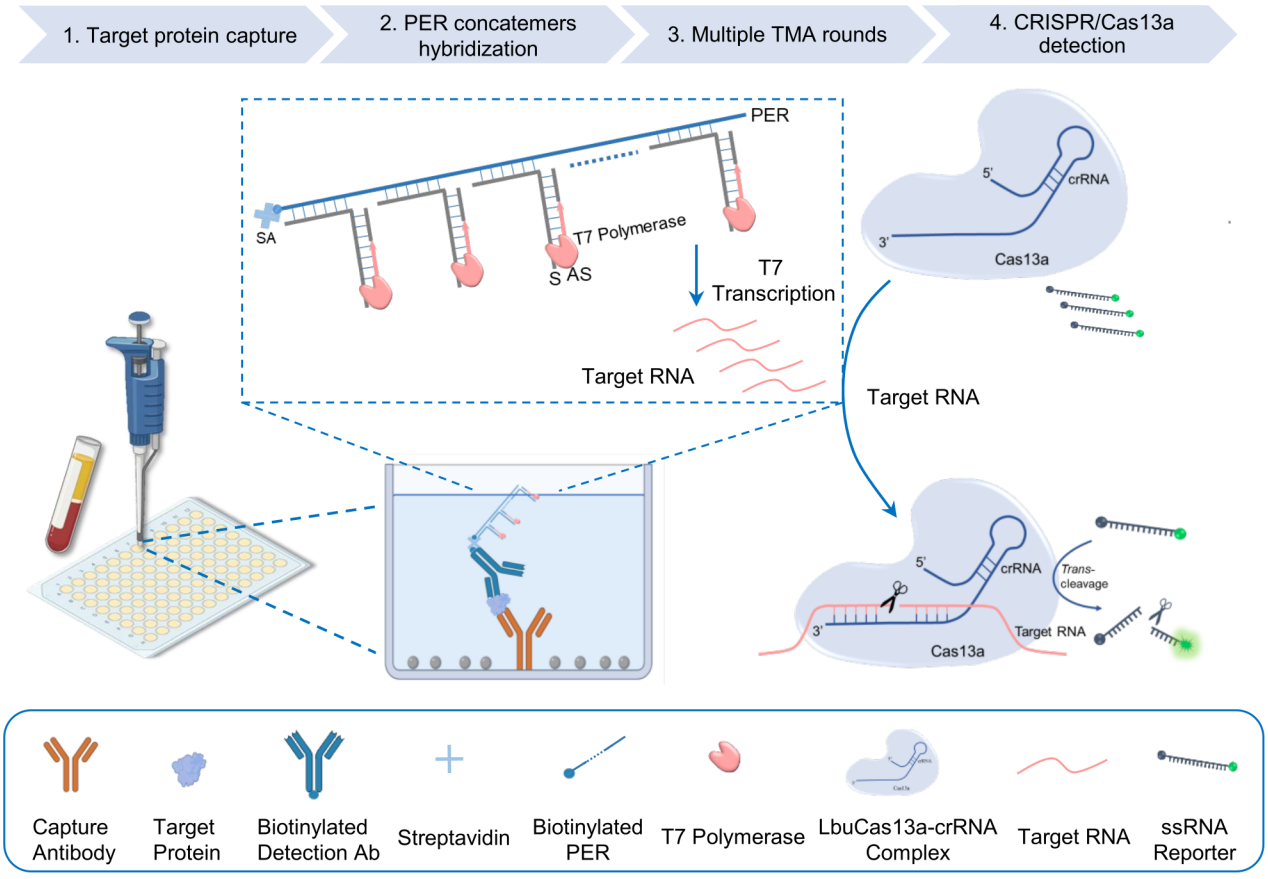


Figure 3 Schematic of iPTC. The target protein is captured by an ELISA double-antibody sandwich structure. After hybridization with AS/S probes containing T7 promoters, long biotinylated repetitive DNA sequences (PER concatemers) bind to the antigen-antibody complex. Then, multiple TMA rounds are performed to generate a mass of target RNA, recognized by crRNA, and trigger transcleavage by Cas13a, resulting in a significant fluorescence signal. AS/S, antisense strand/sense strand; iPTC, immuno-PER-TMA-CRISPR/Cas13a; PER, primer exchange reaction; TMA, transcription-mediated amplification.

flexibly applied to various proteins by simply replacing the antibodies.

To demonstrate the feasibility of this platform, we first expressed and purified the LbuCas13a protein, followed by enzyme activity detection. The molecular weight of our purified LbuCas13a was approximately 130 kD (online supplemental figure 2A). We further tested cleavage activity using target RNA and crRNA selected from our previous study.[29] An elevated fluorescence signal was obtained only when the target RNA and crRNA were both present (online supplemental figure 2B,C), and the LOD was 1.01 pM (online supplemental figure 2D, LOD=3σ/S, where σ is the blank SD, and S is the linear slope). These results validated the enzyme activity of the CRISPR/Cas13a system.

Next, we tested the feasibility of this platform in a heterogeneous manner using SA@MBs (figure 4). The schematic is illustrated in figure 4A. One 3a concatemer could theoretically hybridize with one AS/sense strand (AS/S) probe before SA@MBs captured it. Then, the unbound 3a and AS/S probes could be washed off. AS/S probes with the T7 promoter can initiate T7 transcription to generate numerous target RNAs. These target RNAs activated the Cas13a enzyme, and the fluorescence signal showed a linear dependence on the logarithm of the 3a concentration from 62.5 to 2500 fM. The regression equation was determined to be FI=27 467×lgC-40374 (R^2=0.990) with an LOD of 1.02 fM (figure 4A), which indicated that this approach was 1000-fold more sensitive than the CRISPR/Cas13a system.

We introduced a PER concatemer, a long repetitive strand DNA with more binding sites for T7 promoters to enable further sensitivity enhancement for proteins with relatively low abundance. The mechanism of the PER cycle is illustrated in figure 4B, and it outputs arbitrary ssDNA concatemers through a simple four-step process. As shown in figure 4C, PER products exhibited an obvious single band in lane 1 in the presence of Bst DNA polymerase, a primer, and a hairpin. Moreover, PER sequences were gradually extended over time, and by controlling the time precisely at 120 min (figure 4D), 2500-nt PER products containing approximately 125 repeated binding sites for the T7 promoter probes could be produced. Given that PER extension size is sequence dependent, we tested four pairs of previously reported primers and corresponding hairpin sequences (online supplemental table 1).[39] As shown in online supplemental figure 3A, the apparent band and highest yield were observed in the lane 3 PER

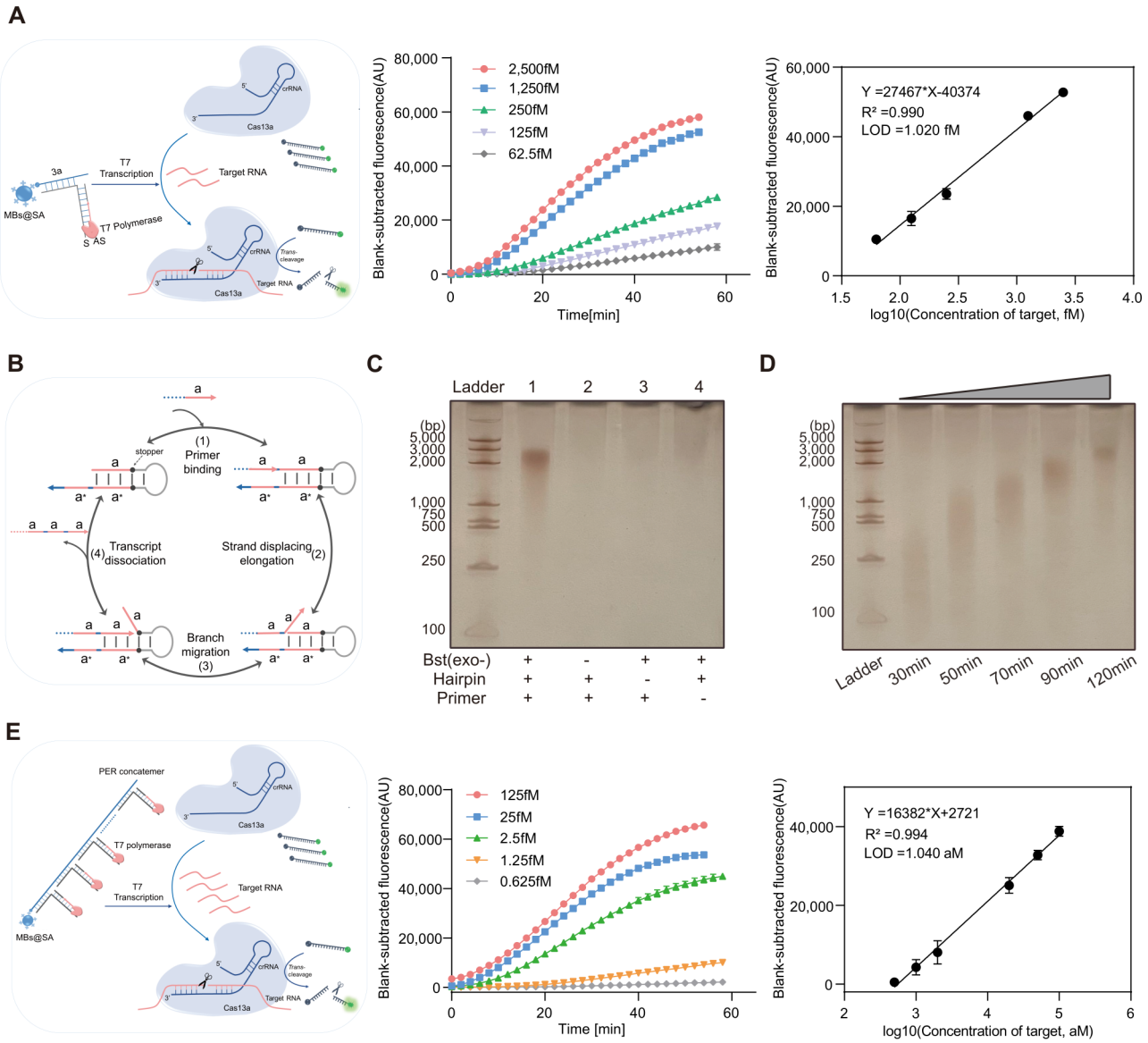


Figure 4 The feasibility of the PTC platform performed on magnetic beads. (A) Schematic for the principle of short-strand target DNA (3a)-activated LbuCas13a after T7 transcription on streptavidin-conjugated magnetic beads (left). The real-time fluorescence kinetics measurements of CRISPR/Cas13a reactions with 3a concentrations ranging from 62.5 to 2500 fM (middle). The sensitivity of CRISPR/Cas13a reactions with 3a (right). (B) Schematic for the primer exchange reaction (PER) cycle principle. (C) The feasibility of the PER reaction was verified by urea-PAGE. (D) The length of PER products was monitored in real-time by urea-PAGE. (E) Schematic for the principle of the long-strand target DNA (PER concatemer)-activated CRISPR/Cas13a system after T7 transcription on streptavidin-conjugated magnetic beads (left). The real-time fluorescence kinetics measurements of CRISPR/Cas13a reactions with PER concatemer concentrations ranging from 0.625 to 125 fM (middle). The sensitivity of CRISPR/Cas13a reactions with PER concatemers (right). Blank-subtracted fluorescence was calculated by subtraction of blank fluorescence values. Error bars represent the SD for three independent experiments. Data are represented as the mean±SD, n=3, three technical replicates. LOD, limit of detection; PTC, PER-TMA-CRISPR/Cas13a.

products, so primer a and hairpin aa were optimal and selected for further assessments. To avoid the influence of a biotinylated primer and hairpin in the PER product mixture, we used a DNA cycle pure kit to wash off the short oligos and collect the long PER products (online supplemental figure 3B).

Subsequently, we replaced 3a with 2500-nt PER concatemers and then hybridized them with AS/S probes (figure 4E). In theory, 125 pairs of AS/S probes could hybridize with the repeated binding sites (5'-CAACTTAACACAACTTAAA-3') on a 2500-nt PER concatemer. After the PER concatemers hybridized with the AS/S probes, T7 transcription was initiated, and the RNA products were subsequently detected by the CRISPR/Cas13a system. The fluorescence signal was found to be linearly dependent on the logarithm of the PER concentration from 0.625 to 125 fM, and the regression equation was determined to be FI=16382×lgC+2721 (R^2=0.994) with an LOD of 1.04 aM; thus, a more than 1000-fold increase in sensitivity was obtained with the

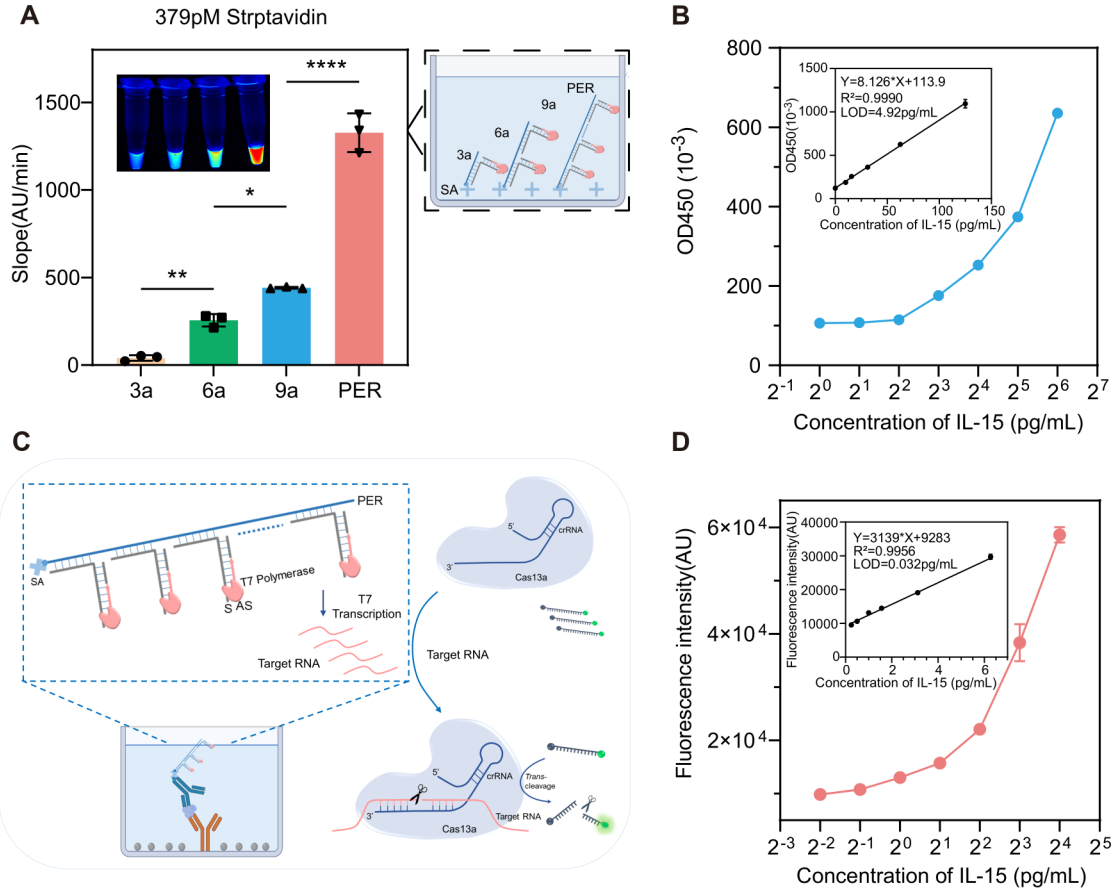


Figure 5 The feasibility of the iPTC platform performed on an ELISA plate. (A) The curve slope and visual fluorescence of the CRISPR/Cas13a reaction on an ELISA plate. The top-right inset demonstrates the schematic for the principle of PTC performed on an ELISA plate, that is, 379 pM streptavidin is precoated on a 96-well plate, and 500 pM different lengths of biotinylated DNA concatemers (3a, 6a, 9a, and PER) hybridized with AS/S probes were bound for subsequent T7 transcription. The slope of the curve over 1 hour was calculated by performing a simple linear regression of data merged from three replicates and is shown as the slope±95% CI. The slopes were compared with the former group by the Kruskal-Wallis test followed by Dunnett's multiple-comparison test: *p<0.05, **p<0.01, ****p<0.0001, respectively. The top-left insert demonstrates the fluorescence intensity of the CRISPR/Cas13a system observed under ultraviolet radiation-based visual readouts, and the tubes from left to right are 3a, 6a, 9a, and PER. (B) The corresponding curve between the IL-15 concentrations and the absorbance at 450 nm was measured by ELISA. The insert shows the linear relationship between absorbance and the concentrations of IL-15, with a LOD of 4.92 pg/mL. (C) Schematic of the principle of iPTC. (D) The corresponding curve between the IL-15 concentrations and the fluorescence intensity measured by iPTC. The insert shows the linear relationship between fluorescence intensity and the concentrations of IL-15, with an LOD of 0.032 pg/mL. Error bars represent the SD for three independent experiments. Data are represented as the mean±SD, n=3, three technical replicates. AS/S, antisense strand/sense strand; iPTC, antisense strand/sense strand; LOD, limit of detection; PER, primer exchange reaction.

long PER concatemers (2500 nt) compared with the short 3a concatemers (30 nt).

Since plate-based ELISA is simpler and more convenient for serum protein detection than magnetic bead-based ELISA, we further evaluated the feasibility of this platform in a heterogeneous assay format using a 96-well plate coated with 379 pM streptavidin. The expected amplification trend was obtained with increasing concatemer length, and the FI showed a sharp increase as the ssDNA length increased in size from 3a to 6a, 9a, and PER (figure 5A). All these results confirmed that PER concatemers greatly improved sensitivity by providing more binding sites for T7 promoters and that this strategy was compatible with both magnetic beads and an ELISA plate.

The detection performance of the iPTC platform

The performance of the iPTC platform, including sensitivity, reproducibility, specificity, correlation, and universality, was assessed. First, we optimized the experimental conditions, and the details are shown in online supplemental figure 4. The range and sensitivity of this platform and the ELISA method were analyzed using the IL-15 standard, and the principle of iPTC is shown in figure 5C. As shown in figure 5B, there was a linear trend in the range of 8–125 pg/mL using a human IL-15 ELISA kit, and the LOD was calculated to be 4.92 pg/mL. As shown in figure 5D, as the concentration of IL-15 increased from 0.25 pg/mL to 16 pg/mL, the FI also increased, and the linear relationship between FI and the concentration of the IL-15 standard could be described as

FI=3139×C+9283, with an LOD of 0.032 pg/mL; this LOD was 153-fold lower than that of the ELISA method. In addition, to evaluate the stability of the iPTC platform, the detection of 0.5 pg/mL and 5 pg/mL IL-15 was repeated five times under identical conditions. As shown in online supplemental table 5, the relative SDs from the mean value were 3.69% and 3.07% for 0.5 pg/mL and 5 pg/mL IL-15, respectively, indicating that the iPTC platform had good reproducibility. Based on this calibration curve, the concentrations of IL-15 in human serum were successfully detected by the iPTC platform with high recovery rates (93.6%–102.0%) (online supplemental table 6).

Other interleukins and proteins (IL-12, IL-7, IL-18, and BSA) were added as interferents to test the analytical specificity of IL-15 in the iPTC platform. Online supplemental figure 5 shows that targeting only IL-15 induced a significant fluorescence increase; even though other interleukins and proteins were used at a concentration 10 times higher than that of IL-15, they did not influence the fluorescence signal. These results indicated that the iPTC platform had excellent specificity due to the specific binding between the antibody and antigen.

We assessed the consistency between the ELISA and iPTC platforms in measuring the sIL-15 levels in 62 NPC patients from group 1. Nonetheless, sIL-15 in most NPC patients (42/62) was below the ELISA's minimum detection limit (LOD=4.92 pg/mL). Hence, we selected the sIL-15 levels detected by ELISA and iPTC methods in 20 NPC patients (sIL-15 levels>4.92 pg/mL) and compared the correlation (online supplemental figure 6A). In the Bland-Altman assay, most results were within the 1.96 SD, indicating that the iPTC platform had great consistency with the ELISA method (online supplemental figure 6B). Furthermore, the equation derived from simple linear regression analysis was Y=0.88X, indicating a high consistency between the two methods (online supplemental figure 6C).

Finally, the universal applicability of this platform was evaluated by detecting another target: the human IL-2 standard. The absorbance (online supplemental figure 7A) and FI (online supplemental figure 7B) increased obviously with increasing concentrations of the target IL-2. In the range from 62.5 fg/mL to 31.2 pg/mL, a linear correlation between FI and the logarithm of the IL-2 concentration was observed. The linear regression equation was determined to be FI=19 011×lgC+36 767 (R^2=0.974), and the LOD was calculated to be 48 fg/mL; this LOD was 100-fold more sensitive than that of ELISA (LOD=4.96 pg/mL).

Baseline sIL-15 level correlates with chemoimmunotherapy response and is associated with progression-free survival in NPC patients

We recruited 130 R/M NPC patients who received chemoimmunotherapy and randomly divided them into a training cohort (n=87) and a validation cohort (n=43). The patient baseline characteristics of the training and validation cohorts are shown in online supplemental table 3. The median follow-up was 17.5 months (IQR 13.9–23.7) and 14.2 months (IQR 10.0–17.9) in the training and validation cohorts, respectively.

Baseline sIL-15 levels on iPTC were significantly higher in the non-PD group (n=65; median, 8.16; IQR, 4.79–13.17; mean, 9.83) in the training cohort than in the PD group (n=22; median, 1.80; IQR, 0–4.16; mean, 3.04; p<0.0001) (figure 6A). A significant difference was also observed in the validation cohort (non-PD: n=31; median, 5.45; IQR, 2.96–7.97; mean, 6.67. PD: n=12; median, 2.34; IQR, 0.53–3.29; mean, 2.66, p<0.0001) (figure 6B). The AUC for sIL-15 was 0.882 (95% CI 0.792 to 0.971, p<0.0001) (figure 6C), and a similar predictive accuracy was obtained in the validation cohort (AUC 0.898, 95% CI 0.771 to 1.000, p<0.0001; figure 6D). The optimal cut-off value (2.90 pg/mL) for IL-15 was used to categorize NPC patients into high-expression and low-expression groups. The patients in the training cohort (n=87) with lower sIL-15 levels (n=19) had a median progression-free survival (PFS) time of 9.8 months, whereas those with higher sIL-15 levels (n=68) had an undefined median PFS time measured in months (HR 0.080, 95% CI 0.027 to 0.239, p<0.0001) (figure 6E). Similar results were observed in the validation patient cohort (n=43); the patients with lower sIL-15 levels (n=9) had a median PFS time of 8.4 months, whereas those with higher sIL-15 levels (n=34) had an undefined median PFS time measured in months (HR 0.053, 95% CI 0.010 to 0.275, p<0.0001) (figure 5F). Mixing all patients, the correlation between sIL-15 levels and ICI response remained significant, supporting the strength of this biomarker (online supplemental figure 8).

Subsequently, we investigated baseline sIL-15 levels in 130 R/M NPC patients using both ELISA and the iPTC platform and compared the predictive performance of sIL-15 assessed by two different methods. The scatter plots (online supplemental figure 9A,B) showed that baseline sIL-15 levels measured by the iPTC (p<0.0001) platform were significantly higher in the non-PD group than in the PD group, with similar results assessed by the ELISA platform (p<0.001). The predictive accuracy of the sIL-15 improved when applied in the iPTC platform (red line, AUC=0.882, 95% CI 0.808 to 0.956, p<0.0001) compared with ELISA (blue line, AUC=0.693, 95% CI 0.60 to 0.78, p=0.0009). Moreover, despite comparable sensitivity and NPV values, the iPTC group had dramatically elevated specificity and PPV than the ELISA group in assessing ICI predictive accuracy. Overall, iPTC enables sIL-15 to serve as a prominent predictor of ICI response.

DISCUSSION

Here, we describe a highly sensitive method for sIL-15 detection using triple signal amplification involving PER, TMA, and the CRISPR/Cas13a system, improving sensitivity by 153-fold compared with ELISA. We also validated the robust predictive effect of baseline sIL-15 for ICI-based treatment in R/M NPC using 130 clinical samples in two

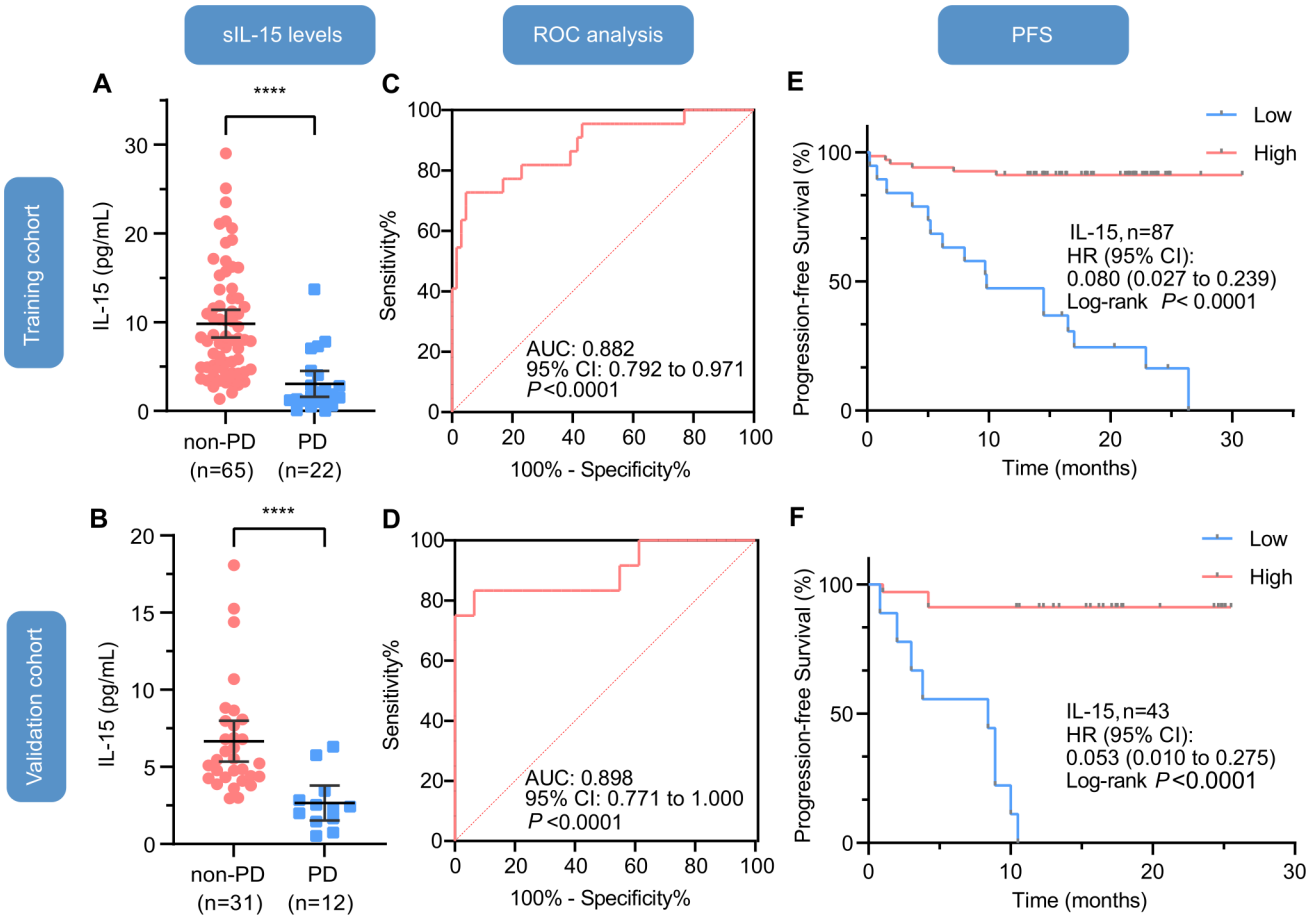


Figure 6 The anti-PD-1 treatment response and outcome prediction based on baseline sIL-15 levels. (A, B) Scatter plots of sIL-15 levels in non-PD patients and PD patients in the training cohort and validation cohort determined by the iPTC platform. The two groups were statistically compared by the Mann-Whitney U test: ****p<0.0001, respectively. (C, D) ROC curve analysis evaluating the predictive power of baseline sIL-15 in differentiating PD patients from non-PD patients, with the corresponding area under the curve in the training and validation cohorts. (E) (F) Baseline sIL-15 levels measured prior to anti-PD-1 therapy were associated with PFS in NPC patients in the training and validation cohorts. Data were analyzed using the log-rank test. iPTC, immuno-PER-TMA-CRISPR/Cas13a; NPC, nasopharyngeal carcinoma; PD, progressive disease; PFS, progression-free survival; ROC, receiver operating characteristic; sIL-15, serum interleukin-15.

independent groups collected from subjects who received both PD-1 inhibitor monotherapy and chemotherapy.

The combination of PD-1/PD-L1 blockade and current treatments has improved the outcomes of patients with R/M NPC.[44] Despite substantial advancements in clinical care, only a small subset of patients with R/M NPC achieve long-lasting clinical benefits from immunotherapy. Given the potential for adverse reactions to immunotherapy, identifying biomarkers that can predict the response to ICIs is of paramount importance. PD-L1 expression,[45] plasma Epstein-Barr virus DNA load,[46–48] and tumor mutational burden (TMB)[46 47] have been investigated in several NPC clinical trials. However, they have not been demonstrated to have a statistically significant clinical predictive value for immunotherapy in NPC, and further exploration is warranted. Recently, the levels of cytokines, such as IL-8, have been considered useful biomarkers across malignancies as predictive factors for immunotherapy response in the context of ICI-based therapy.[2 3 49] Moreover, IL-2,[50 51] IL-12,[52–54] and IL-15[8 55] can induce the proliferation of activated T cells, activate B cells, and enhance the cytotoxic activity of NK cells, thus showing great potential to predict immunotherapy efficacy. In this study, we first explored the roles of IL-8, IL-2, IL-12, and IL-15 as biomarkers for predicting the immune response in NPC and found that sIL-15 showed optimal predictive performance for NPC. Since IL-8 directly reflects changes in the tumor burden, differential expression of IL-8 in NPC and other tumors may account for the variation in results.[9] IL-15 is more similar to an advanced version of IL-2, and the distribution of cell sources and target cells is wider than that of IL-2, thus leading to stronger immune-enhancing effects and superior predictive value.

Despite the potential predictive value of sIL-15, its concentration is extremely low, and traditional ELISA is not sensitive enough. We constructed an iPTC assay that exceeded the performance of ELISA. First, this method achieved enhanced sensitivity. The major mechanism underlying the improved sensitivity is as follows: (1) during the PER process, long concatemers contained

approximately 125 repeated binding sites for the T7 promoter probes form, resulting in a dramatic increase in sensitivity. (2) Our system introduced TMA, an RNA TMA system, to amplify DNA isothermally and produce RNA amplicons, resulting in a considerable signal increase within 30 min. (3) Cleavage of RNA reporters by the collateral activity of LbuCas13a enhances fluorescence signals and improves sensitivity on target RNA recognition. Second, the isothermal amplification design facilitates using the iPTC assay as a simple and versatile tool for microprotein detection. (1) It avoids a tedious PCR process and requires no sophisticated thermal cycling equipment. (2) Like the ELISA method, iPTC can be performed in most laboratories. (3) The preassembled PER concatemers serve as a universal DNA barcode, enabling the detection of different biomarkers by simply changing the antibodies. These properties render iPTC a potentially suitable solution for sIL-15 detection.

By translating protein signals into nucleic acid signals and incorporating CRISPR technology with nucleic acid amplification strategies, our group successfully conducted a substantial amount of work on improving the sensitivity of ELISA, such as PCR-CRISPR/Cas12a-ELISA, RPA-CRISPR/Cas13a-ELISA, and HCR-CRISPR/Cas12a-ELISA.[15 17 18 56] Nevertheless, each approach has shortcomings when applied to cytokine detection. PCR-CRISPR/Cas12a-ELISA requires complex equipment, and extreme care must be taken to avoid contamination. RPA-CRISPR/Cas13a-ELISA can be used in resource-limited settings; however, RPA reagents are costly, and amplicon contamination risks still exist. HCR-CRISPR/Cas12a-ELISA is an enzyme-free amplification reaction; hence, it has a low cost and lower kinetic efficiency and reproducibility. The proposed iPTC assay is an advance in our long-term exploration; it provides femtogram-level sensitivity while avoiding amplicon contamination with a whole duration time of 5 hours. The balance of sensitivity, simplicity, and speed positions iPTC as the appropriate solution for cytokine detection.

iPTC allows us to explore the predictive relevance of sIL-15 for objective ICI response. Our study first demonstrated that sIL-15 could be applied as a useful biomarker to identify NPC patients who are more likely to respond to this costly therapy, which agrees with the in vivo finding that IL-15 activation sensitizes tumors to PD-1, with improved antitumor and survival benefits.[9] Soluble IL-15/IL-15Rα complexes are currently being investigated in phase II clinical trials for therapeutic efficacy in numerous cancer types[57 58]; they are also being studied in combination with PD-1/PD-L1 blockade. The association between an elevated IL-15 level and a superior response indicated that anti-PD-1 treatment efficacy might be enhanced through an IL-15 superagonist in IL-15-low patients at the time of PD-1 therapy initiation.[9 10] To our knowledge, this is the first study to reveal that the baseline sIL-15 level predicts the efficacy of ICI-based treatment in NPC, and further studies in other tumors remain to be performed.

CONCLUSIONS

In conclusion, we constructed a universal and ultrasensitive iPTC platform to detect serum microproteins. This triple signal amplification strategy produced a high-performance immunoassay for sIL-15 with an ultralow LOD of 0.032 pg/mL, which was 153-fold more sensitive than the LOD of conventional ELISA. Additionally, we proposed for the first time that sIL-15 levels were a potential predictive biomarker for anti-PD-1 treatment in patients with advanced NPC. In addition, we discovered that high baseline sIL-15 levels were associated with longer PFS in NPC patients receiving ICI and chemotherapy. However, our study has several limitations. First, the iPTC assay takes more time than conventional ELISA. Our assay provides higher sensitivity despite the longer reaction time (2 hours). Admittedly, our results should be confirmed in independent larger, multicenter studies. We hope that the construction of this iPTC platform can provide some inspiration for detecting microproteins in clinical samples and for the use of sIL-15 in predicting immunotherapy outcomes.

Author affiliations
[1]Department of Clinical Laboratory, State Key Laboratory of Oncology in South China, Guangdong Key Laboratory of Nasopharyngeal Carcinoma Diagnosis and Therapy, Sun Yat-sen University Cancer Center, Guangzhou 510060, P. R. China
[2]Department of Experimental Research, State Key Laboratory of Oncology in South China, Guangdong Key Laboratory of Nasopharyngeal Carcinoma Diagnosis and Therapy, Sun Yat-sen University Cancer Center, Guangzhou 510060, P. R. China

Acknowledgements We thank the patients at Sun Yat-sen university cancer center for their contribution to this study.

Contributors Y-XW, SX and YW contributed equally to this work. W-LL and M-SZ conceived this study, and they are the corresponding authors. Y-XW, SX and YW designed the experiments, performed most of the experiments, and wrote the draft manuscript. B-YT, X-PW and X-HL provided patient recruitment and sample collection. MW, QH, XH and S-LC provided experience with CRISPR-based diagnostic development and optimized the platform. All the authors read, revised, and approved the manuscript. Guarantors: W-LL and M-SZ.

Funding This study was supported by grants from the National Natural Science Foundation of China (No. 81871711 and No. 82002240) and the Natural Science Foundation of Guangdong Province (2019A1515010798).

Competing interests None declared.

Patient consent for publication Not applicable.

Ethics approval This study involves human participants and the Institutional Review Board of SYSUCC approved this study (B2022-636-01). Participants gave informed consent to participate in the study before taking part.

Provenance and peer review Not commissioned; externally peer reviewed.

Data availability statement Data are available on reasonable request. The datasets used and/or analyzed during the current study are available from the corresponding author on reasonable request.

Supplemental material This content has been supplied by the author(s). It has not been vetted by BMJ Publishing Group Limited (BMJ) and may not have been peer-reviewed. Any opinions or recommendations discussed are solely those of the author(s) and are not endorsed by BMJ. BMJ disclaims all liability and responsibility arising from any reliance placed on the content. Where the content includes any translated material, BMJ does not warrant the accuracy and reliability of the translations (including but not limited to local regulations, clinical guidelines, terminology, drug names and drug dosages), and is not responsible for any error and/or omissions arising from translation and adaptation or otherwise.

Open access This is an open access article distributed in accordance with the Creative Commons Attribution Non Commercial (CC BY-NC 4.0) license, which

permits others to distribute, remix, adapt, build upon this work non-commercially, and license their derivative works on different terms, provided the original work is properly cited, appropriate credit is given, any changes made indicated, and the use is non-commercial. See http://creativecommons.org/licenses/by-nc/4.0/.

ORCID iDs
Xue-Ping Wang http://orcid.org/0000-0002-3519-3100
Wan-Li Liu http://orcid.org/0000-0002-7467-760X

REFERENCES

1 Xu J-Y, Wei X-L, Wang Y-Q, *et al*. Current status and advances of Immunotherapy in Nasopharyngeal carcinoma. *Ther Adv Med Oncol* 2022;14:17588359221096214.
2 Sanmamed MF, Perez-Gracia JL, Schalper KA, *et al*. Changes in serum Interleukin-8 (IL-8) levels reflect and predict response to anti-PD-1 treatment in Melanoma and non-small-cell lung cancer patients. *Ann Oncol* 2017;28:1988–95.
3 Schalper KA, Carleton M, Zhou M, *et al*. Elevated serum Interleukin-8 is associated with enhanced Intratumor neutrophils and reduced clinical benefit of immune-Checkpoint inhibitors. *Nat Med* 2020;26:688–92.
4 Giuffrida L, Sek K, Henderson MA, *et al*. IL-15 Preconditioning augments CAR T cell responses to Checkpoint blockade for improved treatment of solid tumors. *Mol Ther* 2020;28:2379–93.
5 Yu P, Steel JC, Zhang M, *et al*. Simultaneous blockade of multiple immune system inhibitory checkpoints enhances antitumor activity mediated by Interleukin-15 in a murine metastatic colon carcinoma model. *Clin Cancer Res* 2010;16:6019–28.
6 Hailemichael Y, Johnson DH, Abdel-Wahab N, *et al*. Interleukin-6 blockade Abrogates Immunotherapy toxicity and promotes tumor immunity. *Cancer Cell* 2022;40:509–23.
7 Zhou T, Damsky W, Weizman O-E, *et al*. IL-18Bp is a secreted immune Checkpoint and barrier to IL-18 Immunotherapy. *Nature* 2020;583:609–14.
8 Steel JC, Waldmann TA, Morris JC. Interleukin-15 biology and its therapeutic implications in cancer. *Trends Pharmacol Sci* 2012;33:35–41.
9 Kurz E, Hirsch CA, Dalton T, *et al*. Exercise-induced engagement of the IL-15/IL-15Rα axis promotes anti-tumor immunity in Pancreatic cancer. *Cancer Cell* 2022;40:720–37.
10 Zhang M, Yao Z, Dubois S, *et al*. Interleukin-15 combined with an anti-Cd40 antibody provides enhanced therapeutic efficacy for murine models of colon cancer. *Proc Natl Acad Sci USA* 2009;106:7513–8.
11 Desbois M, Le Vu P, Coutzac C, *et al*. IL-15 Trans-signaling with the Superagonist RLI promotes Effector/memory Cd8+ T cell responses and enhances antitumor activity of PD-1 antagonists. *J Immunol* 2016;197:168–78.
12 Cheng L, Du X, Wang Z, *et al*. Hyper-IL-15 suppresses metastatic and autochthonous liver cancer by promoting tumour-specific Cd8+ T cell responses. *J Hepatol* 2014;61:1297–303.
13 Sanjabi S, Mosaheb MM, Flavell RA. Opposing effects of TGF-beta and IL-15 Cytokines control the number of short-lived Effector Cd8+ T cells. *Immunity* 2009;31:131–44.
14 Peng P, Liu C, Li Z, *et al*. Emerging ELISA derived Technologies for in vitro diagnostics. *TrAC Trends in Analytical Chemistry* 2022;152:116605.
15 Niemeyer CM, Adler M, Blohm D. Fluorometric polymerase chain reaction (PCR) enzyme-linked immunosorbent assay for Quantification of Immuno-PCR products in Microplates. *Anal Biochem* 1997;246:140–5.
16 Niemeyer CM, Adler M, Wacker R. Immuno-PCR: high sensitivity detection of proteins by nucleic acid amplification. *Trends Biotechnol* 2005;23:208–16.
17 Sano T, Smith CL, Cantor CR. Immuno-PCR: very sensitive antigen detection by means of specific antibody-DNA conjugates. *Science* 1992;258:120–2.
18 Santiago-Felipe S, Tortajada-Genaro LA, Puchades R, *et al*. Recombinase polymerase and enzyme-linked immunosorbent assay as a DNA amplification-detection strategy for food analysis. *Anal Chim Acta* 2014;811:81–7.
19 Gootenberg JS, Abudayyeh OO, Kellner MJ, *et al*. Multiplexed and portable nucleic acid detection platform with Cas13, Cas12A, and Csm6. *Science* 2018;360:439–44.
20 Gootenberg JS, Abudayyeh OO, Lee JW, *et al*. Nucleic acid detection with CRISPR-Cas13A/C2C2. *Science* 2017;356:438–42.
21 Joung J, Ladha A, Saito M, *et al*. Detection of SARS-Cov-2 with SHERLOCK one-pot testing. *N Engl J Med* 2020;383:1492–4.
22 Liu L, Li X, Ma J, *et al*. The molecular architecture for RNA-guided RNA cleavage by Cas13A. *Cell* 2017;170:714–26.
23 Wang B, Wang R, Wang D, *et al*. Cas12Avdet: A CRISPR/Cas12A-based platform for rapid and visual nucleic acid detection. *Anal Chem* 2019;91:12156–61.
24 Mahas A, Wang Q, Marsic T, *et al*. A novel miniature CRISPR-Cas13 system for SARS-Cov-2 diagnostics. *ACS Synth Biol* 2021;10:2541–51.
25 Abudayyeh OO, Gootenberg JS, Essletzbichler P, *et al*. RNA targeting with CRISPR-Cas13. *Nature* 2017;550:280–4.
26 Fozouni P, Son S, Díaz de León Derby M, *et al*. Amplification-free detection of SARS-Cov-2 with CRISPR-Cas13A and mobile phone microscopy. *Cell* 2021;184:323–33.
27 Li H, Xing S, Xu J, *et al*. Aptamer-based CRISPR/Cas12A assay for the Ultrasensitive detection of extracellular Vesicle proteins. *Talanta* 2021;221:121670.
28 Xing S, Lu Z, Huang Q, *et al*. An Ultrasensitive hybridization chain reaction-amplified CRISPR-Cas12A Aptasensor for extracellular Vesicle surface protein Quantification. *Theranostics* 2020;10:10262–73.
29 He Y, Wu Y, Wang Y, *et al*. Applying CRISPR/Cas13 to construct Exosomal PD-L1 Ultrasensitive Biosensors for dynamic monitoring of tumor progression in Immunotherapy. *Adv Therap* 2020;3:2000093.
30 Chen Q, Tian T, Xiong E, *et al*. CRISPR/Cas13A signal amplification linked immunosorbent assay for Femtomolar protein detection. *Anal Chem* 2020;92:573–7.
31 Kishi JY, Schaus TE, Gopalkrishnan N, *et al*. Programmable autonomous synthesis of single-stranded DNA. *Nat Chem* 2018;10:155–64.
32 Saiki RK, Gelfand DH, Stoffel S, *et al*. Primer-directed enzymatic amplification of DNA with a Thermostable DNA polymerase. *Science* 1988;239:487–91.
33 van Dongen JJ, Breit TM, Adriaansen HJ, *et al*. Detection of minimal residual disease in acute leukemia by immunological marker analysis and polymerase chain reaction. *Leukemia* 1992;6 Suppl 1:47–59.
34 Lizardi PM, Huang X, Zhu Z, *et al*. Mutation detection and single-molecule counting using isothermal rolling-circle amplification. *Nat Genet* 1998;19:225–32.
35 Ali MM, Li F, Zhang Z, *et al*. Rolling circle amplification: a versatile tool for chemical biology, materials science and medicine. *Chem Soc Rev* 2014;43:3324–41.
36 Montagne K, Plasson R, Sakai Y, *et al*. Programming an in vitro DNA oscillator using a molecular networking strategy. *Mol Syst Biol* 2011;7:466.
37 Dai Y, Xu W, Somoza RA, *et al*. An integrated multi-function heterogeneous biochemical circuit for high-resolution Electrochemistry-based genetic analysis. *Angew Chem Int Ed Engl* 2020;59:20545–51.
38 Li X, Li X, Li D, *et al*. Electrochemical Biosensor for Ultrasensitive Exosomal miRNA analysis by Cascade primer exchange reaction and MOF@Pt@MOF Nanozyme. *Biosensors and Bioelectronics* 2020;168:112554.
39 Saka SK, Wang Y, Kishi JY, *et al*. Immuno-SABER enables highly Multiplexed and amplified protein imaging in tissues. *Nat Biotechnol* 2019;37:1080–90.
40 Kishi JY, Lapan SW, Beliveau BJ, *et al*. SABER Amplifies FISH: enhanced Multiplexed imaging of RNA and DNA in cells and tissues. *Nat Methods* 2019;16:533–44.
41 Xie Z, Chen S, Zhang W, *et al*. A novel fluorescence amplification strategy combining Cascade primer exchange reaction with CRISPR/Cas12A system for Ultrasensitive detection of Rnase H activity. *Biosens Bioelectron* 2022;206:114135.
42 Li D, Duan C, Cheng W, *et al*. A simple and rapid method to assay SARS-Cov-2 RNA based on a primer exchange reaction. *Chem Commun (Camb)* 2022;58:4484–7.
43 Chevallet M, Luche S, Rabilloud T. Silver staining of proteins in Polyacrylamide Gels. *Nat Protoc* 2006;1:1852–8.
44 Even C, Wang H-M, Li S-H, *et al*. Phase II, randomized study of Spartalizumab (Pdr001), an anti-PD-1 antibody, versus chemotherapy in patients with recurrent/metastatic Nasopharyngeal cancer. *Clin Cancer Res* 2021;27:6413–23.
45 Shen L, Guo J, Zhang Q, *et al*. Tislelizumab in Chinese patients with advanced solid tumors: an open-label, non-comparative, phase 1/2 study. *J Immunother Cancer* 2020;8:e000437.
46 Fang W, Yang Y, Ma Y, *et al*. Camrelizumab (SHR-1210) alone or in combination with Gemcitabine plus cisplatin for Nasopharyngeal carcinoma: results from two single-arm, phase 1 trials. *Lancet Oncol* 2018;19:1338–50.
47 Wang F-H, Wei X-L, Feng J, *et al*. Efficacy, safety, and correlative biomarkers of Toripalimab in previously treated recurrent or

metastatic Nasopharyngeal carcinoma: A phase II clinical trial (POLARIS-02). *J Clin Oncol* 2021;39:704–12.
48 Yang Y, Qu S, Li J, *et al*. Camrelizumab versus placebo in combination with Gemcitabine and cisplatin as first-line treatment for recurrent or metastatic Nasopharyngeal carcinoma (CAPTAIN-1St): a Multicentre, randomised, double-blind, phase 3 trial. *Lancet Oncol* 2021;22:1162–74.
49 Teijeira A, Garasa S, Ochoa MC, *et al*. Il8, neutrophils, and nets in a collusion against cancer immunity and Immunotherapy. *Clin Cancer Res* 2021;27:2383–93.
50 Fehniger TA, Cooper MA, Caligiuri MA. Interleukin-2 and Interleukin-15: Immunotherapy for cancer. *Cytokine Growth Factor Rev* 2002;13:169–83.
51 Waldmann TA. The biology of Interleukin-2 and Interleukin-15: implications for cancer therapy and vaccine design. *Nat Rev Immunol* 2006;6:595–601.
52 Agliardi G, Liuzzi AR, Hotblack A, *et al*. Intratumoral IL-12 delivery empowers CAR-T cell Immunotherapy in a pre-clinical model of glioblastoma. *Nat Commun* 2021;12:444.
53 Garris CS, Arlauckas SP, Kohler RH, *et al*. Successful anti-PD-1 cancer Immunotherapy requires T cell-Dendritic cell Crosstalk involving the Cytokines IFN-Γ and IL-12. *Immunity* 2018;49:1148–61.
54 Maier B, Leader AM, Chen ST, *et al*. Author correction: A conserved Dendritic-cell regulatory program limits Antitumour immunity. *Nature* 2020;582:E17.
55 Ma S, Caligiuri MA, Yu J. Harnessing IL-15 signaling to potentiate NK cell-mediated cancer Immunotherapy. *Trends Immunol* 2022;43:833–47.
56 Zhang B, Liu B, Tang D, *et al*. DNA-based hybridization chain reaction for amplified Bioelectronic signal and Ultrasensitive detection of proteins. *Anal Chem* 2012;84:5392–9.
57 Conlon K, Watson DC, Waldmann TA, *et al*. Phase I study of single agent Niz985, a recombinant Heterodimeric IL-15 agonist, in adult patients with metastatic or Unresectable solid tumors. *J Immunother Cancer* 2021;9:e003388.
58 Conlon KC, Lugli E, Welles HC, *et al*. Redistribution, Hyperproliferation, activation of natural killer cells and Cd8 T cells, and cytokine production during first-in-human clinical trial of recombinant human Interleukin-15 in patients with cancer. *J Clin Oncol* 2015;33:74–82.